Technical Report

Demonstration of Advanced EMI Models for Live-Site UXO Discrimination at Waikoloa, Hawaii

ESTCP Project MR-201227

December 2015

Fridon Shubitidze
White River Technologies, Inc.

ESTCP

REPORT DOCUMENTATION PAGE

1. REPORT DATE *(DD-MM-YYYY)*	2. REPORT TYPE	3. DATES COVERED *(From - To)*
12/15/2015	Technical Report	February - December, 2015

4. TITLE AND SUBTITLE

DEMONSTRATION OF ADVANCED EMI MODELS FOR LIVE-SITE UXO DISCRIMINATION AT WAIKOLOA, HAWAII

5a. CONTRACT NUMBER
W912HQ- 12-C-0056

5b. GRANT NUMBER

5c. PROGRAM ELEMENT NUMBER

6. AUTHOR(S)

Dr. Fridon Shubitidze
Thayer School of Engineering, Dartmouth College
14 Engineering Drive
Hanover, NH 03750

5d. PROJECT NUMBER
MR-201227

5e. TASK NUMBER

5f. WORK UNIT NUMBER

7. PERFORMING ORGANIZATION NAME(S) AND ADDRESS(ES)

White River Technologies, Inc.
115 Etna Road, Building 3, Suite 1
Lebanon, NH 03766

8. PERFORMING ORGANIZATION REPORT NUMBER

9. SPONSORING / MONITORING AGENCY NAME(S) AND ADDRESS(ES)

Environmental Security Technology Certification Program (ESTCP)
4800 Mark Center Drive
Suite 17D08
Alexandria VA 22350-3600

10. SPONSOR/MONITOR'S ACRONYM(S)
ESTCP

11. SPONSOR/MONITOR'S REPORT NUMBER(S)

12. DISTRIBUTION / AVAILABILITY STATEMENT

Approved for public release; distribution is unlimited.

13. SUPPLEMENTARY NOTES
N/A

14. ABSTRACT

This report describes in detail the procedures and approaches WRT Inc. team took to complete an Environmental Security Technology Certification Program (ESTCP)-funded live-site UXO demonstration study at the former Waikoloa Maneuver Area (WMA) in Waikoloa, Hawaii, under ESTCP Munitions Response Project MR-201227.

15. SUBJECT TERMS

16. SECURITY CLASSIFICATION OF:			17. LIMITATION OF ABSTRACT	18. NUMBER OF PAGES	19a. NAME OF RESPONSIBLE PERSON
a. REPORT U	**b. ABSTRACT** U	**c. THIS PAGE** U	SAR	44	Dr. Fridon Shubitidze
					19b. TELEPHONE NUMBER *(include area code)* 603-646-3671

List of Figures

List of Tables

List of Acronyms

AL	Alabama
APG	Aberdeen Proving Ground
CA	California
cm	Centimeter
DE	Differential evolution
DLL	Dynamic Link Libraries
DoD	Department of Defense
EMI	Electromagnetic Induction
ESTCP	Environmental Security Technology Certification Program
HI	Hawaii
IDA	Institute for Defense Analys**e**s.
Inc	Incorporated
JD	Joint Diagonalization
μs	Microsecond
mm	Millimeter
MM	MetalMapper
MPV	Man-Portable Vector
ms	Millisecond
MSR	Multi-static response
NC	North Carolina
NSMS	Normalized surface magnetic source
NV/SMS	Normalized volume or surface magnetic source models
ONVMS	Orthogonal normalized volume magnetic source
ONV/SMS	Orthonormalized volume or surface magnetic source models
PNN	Probabilistic Neural Network
SERDP	Strategic Environmental Research and Development Program
SLO	San Luis Obispo
SNR	Signal to noise ratio
SVM	Support vector machine
TD	Time Domain
TEMTADS	Time Domain Electromagnetic Towed Array Detection System
TOI	Target of Interest
TONVMS	Total Orthonormalized volume magnetic source
Tx/Rx	Transmitter / Receiver
UXO	Unexploded Ordnance
WMA	Waikoloa Maneuver Area
WRT	White River Technology

1.0 Exclusive Summary

This report describes in detail the procedures and approaches WRT Inc. team took to complete an Environmental Security Technology Certification Program (ESTCP)-funded live-site UXO demonstration study at the former Waikoloa Maneuver Area (WMA) in Waikoloa, Hawaii, under ESTCP Munitions Response Project 201227. The main objectives of this demonstration study at the former WMA were:

1. Test the discrimination capability of the advanced EMI models for live-site conditions in the presence of magnetically susceptible soils.
2. Validate technology by inverting the target's intrinsic parameters and identifying robust classification features, which distinguish UXO targets from non-hazardous objects.
3. Document the applicability and limitations of the advanced EMI discrimination technologies for magnetically susceptible soils.

Parsons delivered all WMA cued (1032) and site specific background data set to us. All data were processed using our advanced, electromagnetic induction (EMI) models, such as orthonormalized volume magnetic source (ONVMS), joint diagonalization (JD) and differential evolution (DE) approach. Our studies showed that the ONVMS method is able to separate targets responses from magnetic soil responses without any difficulties when the distance between target and sensor is less than 30 cm. The prioritized dig list was generated and submitted to the ESTCP office and scored against the ground truth from the intrusive investigation. Two seed items were incorrectly classified as nonhazardous clutter. Failure analysis indicated that the incorrect classification was due to the combination of lateral offset, strong geological background responses and breakdown of one of the receiver cubes. Namely, misclassification of one of the two targets was due to significant (43 cm) offset between the MM data collection point and the actual location of the seed. The second incorrect classification appeared to be a result of combination of: a) the large offset (27.86 cm) between the MM center and the seed target, and b) being the completely failed Rx cube (Rx#0) adjacent to the actual seed target. We believe, that having a robust in-field or off-line quality check step could guide an operator to place the sensor close to the anomaly, collect high quality data and avoid these misclassifications in challenging sites, such as WMA.

Comparisons between our classification and Parsons intrusive investigation results revealed significant discrepancies. For example, Parsons considered anomalies #29, 36, 199, 441, and 442 as "no contacts", however MM data and our classification results show with high confidence that these anomalies were compact, 37 mm projectiles and 60 mm mortar like metallic targets. These discrepancies indicate that the intrusive procedure, which was used by Parsons at WMA, failed to document accurately all intrusive results, or failed to detect and clear all UXO like targets on the site. Thus, for cleaning UXO sites reliably and effectively the classification results must be used to guide and validate intrusive investigation results.

2.0 INTRODUCTION

This demonstration is designed to illustrate discrimination performance of advanced, electromagnetic induction (EMI) models, such as orthonormalized volume magnetic source (ONVMS) [1], joint diagonalization (JD) and differential evolution (DE) approach [2], [3]-[5], at the former Waikoloa Maneuver Area (WMA), Hawaii, as a part of ESTCP live-site UXO classification pilot studies program. The site – located on the northwest side of the Island of Hawaii, approximately 30 miles north of the city of Kailua-Kona in the South Kohala District – was acquired by the Navy in 1943 and used as a military training camp and artillery range for 50,000 troops until 1945. The advanced EMI models used here have been developed under the SERDP MM-1572 project and successfully applied to the next generation EMI sensor's [6]-[12] datasets collected at the Camp Sibert, AL, the Aberdeen Proving Ground (APG), San Luis Obispo, CA[7], Camp Butner, NC [9], [13] and Camp Beale, CA [10] live sites. In this demonstration the models are applied to data collected using the Metal Mapper (MM) instrument. The suspected munitions at the site are 60-mm and 80-mm high explosive mortars, 75-mm, 105-mm, and 155-mm projectiles, 2.36-inch rocket propelled anti-tank rounds, US MK II hand grenades, Rockets, M1 anti-tank land mines, and Japanese ordnance. During WMA MM data analysis and classification study, for each anomaly, MM data are inverted and the targets intrinsic (total volume magnetic source (NVMS) i.e. the size, shape and material properties) and extrinsic (location, depth, orientation) parameters are estimated. The intrinsic parameters are used for classification and a ranked dig-list is generated. The dig-list is submitted to the Institute for Defense Analyses (IDA) for independent scoring. The advanced models classification performances are assessed and documented based on the independently scored results.

2.1 Objective of the Demonstration

The principal objectives of this project are to apply advanced EMI models to UXO discrimination problems on live sites and to demonstrate classification capability under real world scenarios. Specific technical objectives are to:

4. Demonstrate the discrimination capability of the advanced EMI models for live-site conditions;
5. Invert the target's intrinsic parameters, and identify robust classification features, which distinguish UXO targets from non-hazardous objects. Namely, the technology should:
   a. Identify all seeded and native UXO.
   b. Eliminate at least 75% of targets that do not correspond to targets of interests (TOI).
6. Identify sources of uncertainty in the classification process and include them in a dig/no-dig decision process;
7. Understand and document the applicability and limitations of the advanced EMI discrimination technologies in the context of project objectives, site characteristics, and suspected ordnance contamination.

3.0 TECHNOLOGY

The advanced EMI models with a statistical signal processing approach, developed and tested over the past six years as part of SERDP MM-1572, showed excellent discrimination performance when applied to next-generation-sensor data collected at various live sites, such as Camp Sibert, Al, San Louis Obispo (SLO), CA, Camp Butner, NC and Camp Beale, as well as APG test sites. The technology was able to single out UXO ranging in caliber from 25 mm up to 155 mm. The ONVMS/JD technique, moreover, was seen to provide excellent classification in both single and multiple-target scenarios when combined with multi-axis/transmitter/receiver sensors like TEMTADS [1] and the MM [6]. The methodology, augmented to include a suite of classifiers, was also adapted to handheld sensors like the MPV and 2x2-3D TEMTADS [12].Recent classification studies showed that not only were the advanced EMI models able to classify all "easy seed UXO items," they also managed to identify all other targets, no matter how unexpected or site-specific, and as small as 3-cm fuzes [11]. Detailed Description of data inversions, targets feature clustering and selections and classicization using the ONVMS, JD, DE and Gaussian mixture model approaches are documented in reports [11], [28], and peer-reviewed publications [5], [14], [15], [29].

3.1.1 WMA MM data inversion and classification scheme

The MM sensor's Tx and Rx signals detailed modeling approach using the ONVMS-DE algorithm is described in [11].

Step 1. Data pre-processing: All MM data were pre-processed using a Matlab Code (see Appendixes in [11]). The code reads comma-delimited format CSV files, subtracts backgrounds from data and transfers them to ASCII files compatible with the ONVMS-DE code (ONVMS_MM.exe). The user needs only to specify the path to the folder with the CSV files; the code then converts them all and prepares for inversion.

Step 2. Create MM Multi Static Response (MSR) data matrix: Using procedures described in [11], we construct the measurement matrix $\bar{\bar{H}}(t_q)$ for each anomaly and use it to create the MM MSR data matrix.

Step 3. Eigenvalue analysis: The JD technique is applied to the created MM MSR data matrix to extract the time-dependent eigenvalues for each anomaly. The eigenvalues for some of the WMA seeded anomalies and soils are depicted in Figure 1 and Figure 2. The MSR data matrix eigenvalues are intrinsic properties of the targets; each target has at least three eigenvalues above the threshold (noise level: low magnitude eigenvalues). For example, Figure 1 shows the eigenvalues extracted for a 37mm projectile, a small ISO, a 60 mm mortar and a 81 mm projectile, and Figure 2 shows eigenvalues vs time for soils. The results illustrate that each target has distinguishable eigenvalues that can be used for classification; Note that the magnitudes of the MSR eigenvalues depend on the depths and orientations of the targets [2]; therefore, the user should use only their shapes when performing classification. In this study, we examined the eigenvalues versus time for each case and used them to estimate the number of sources and SNR. Once we had the JD

analysis and estimated SNR for each anomaly we proceeded to invert all cued MM datasets using the combined ONVMS-DE algorithm for multi-targets.
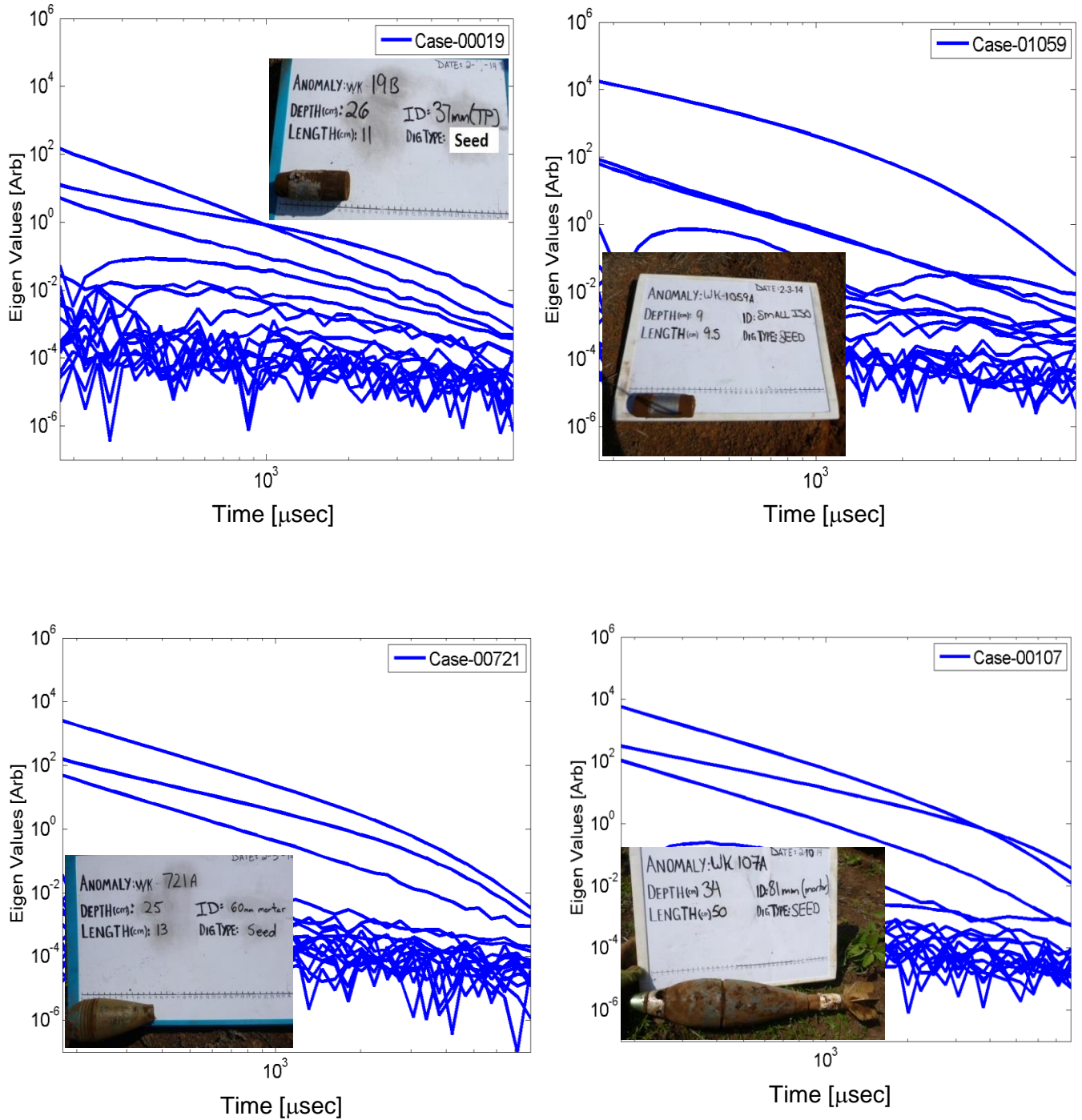
Figure 1. WMA MM multi-static response matrix eigenvalues versus time for some samples of seeded anomalies.
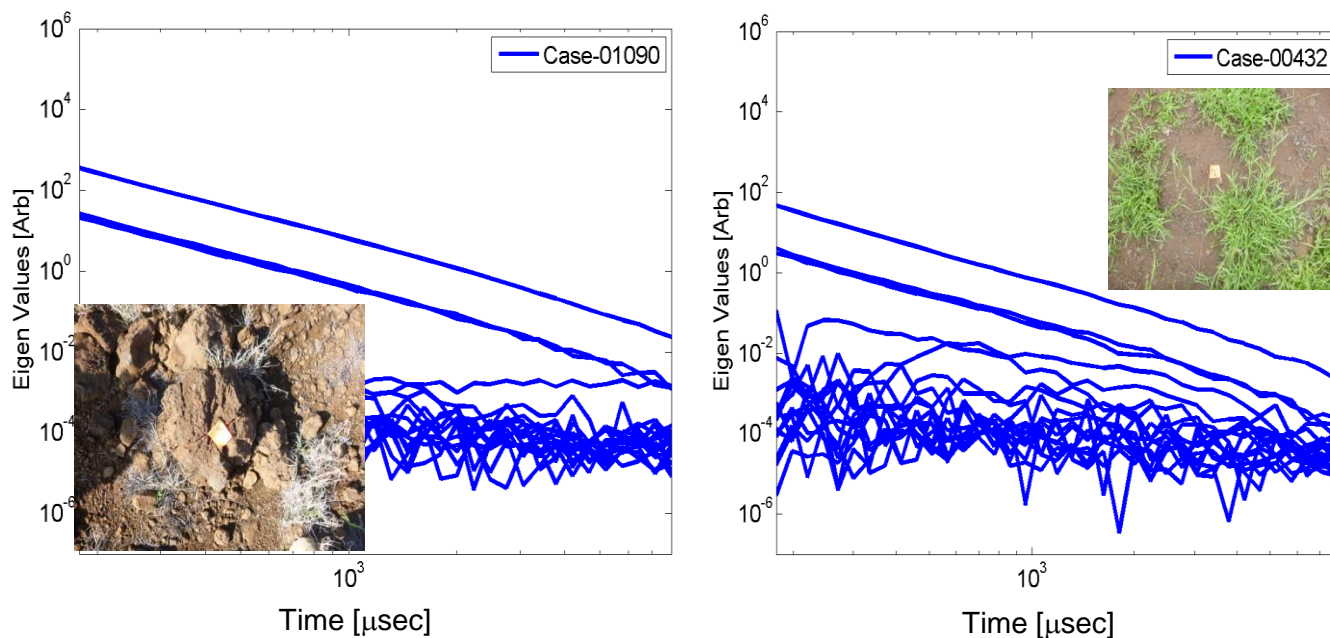
Figure 2. MM multi-static response matrix eigenvalues versus time for some samples of WMA soils.
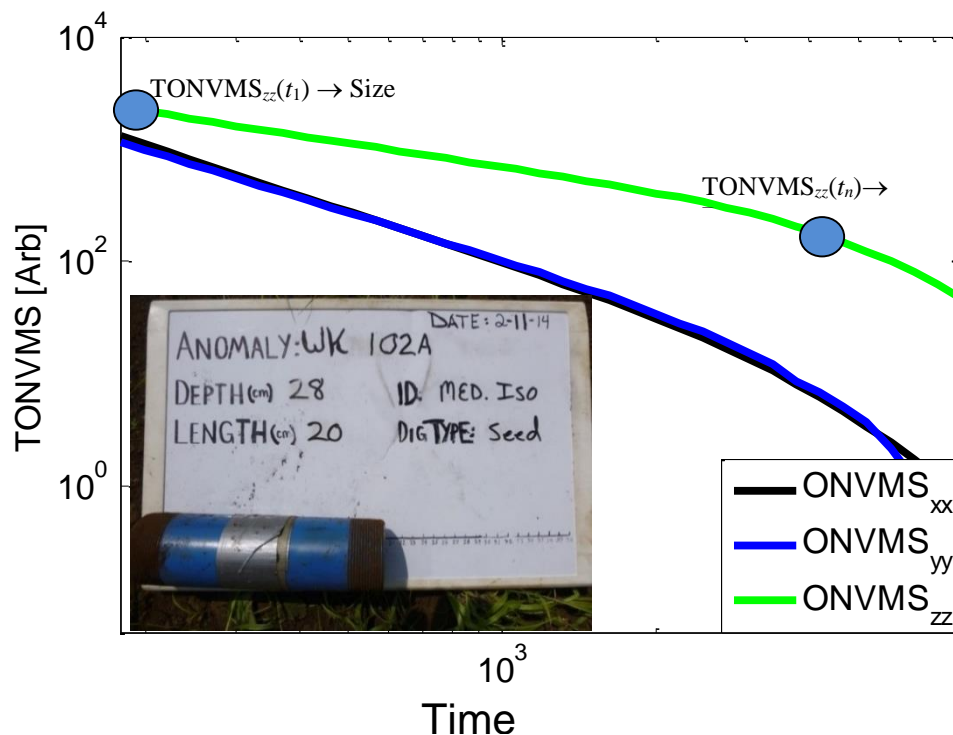
Figure 3. Inverted total ONVMS time-decay profiles for a WMA medium ISO target.

Step 4. Extract the total ONVMS for each anomaly. The targets' extrinsic and intrinsic parameters, including the total ONVMS where extorted for all anomalies.
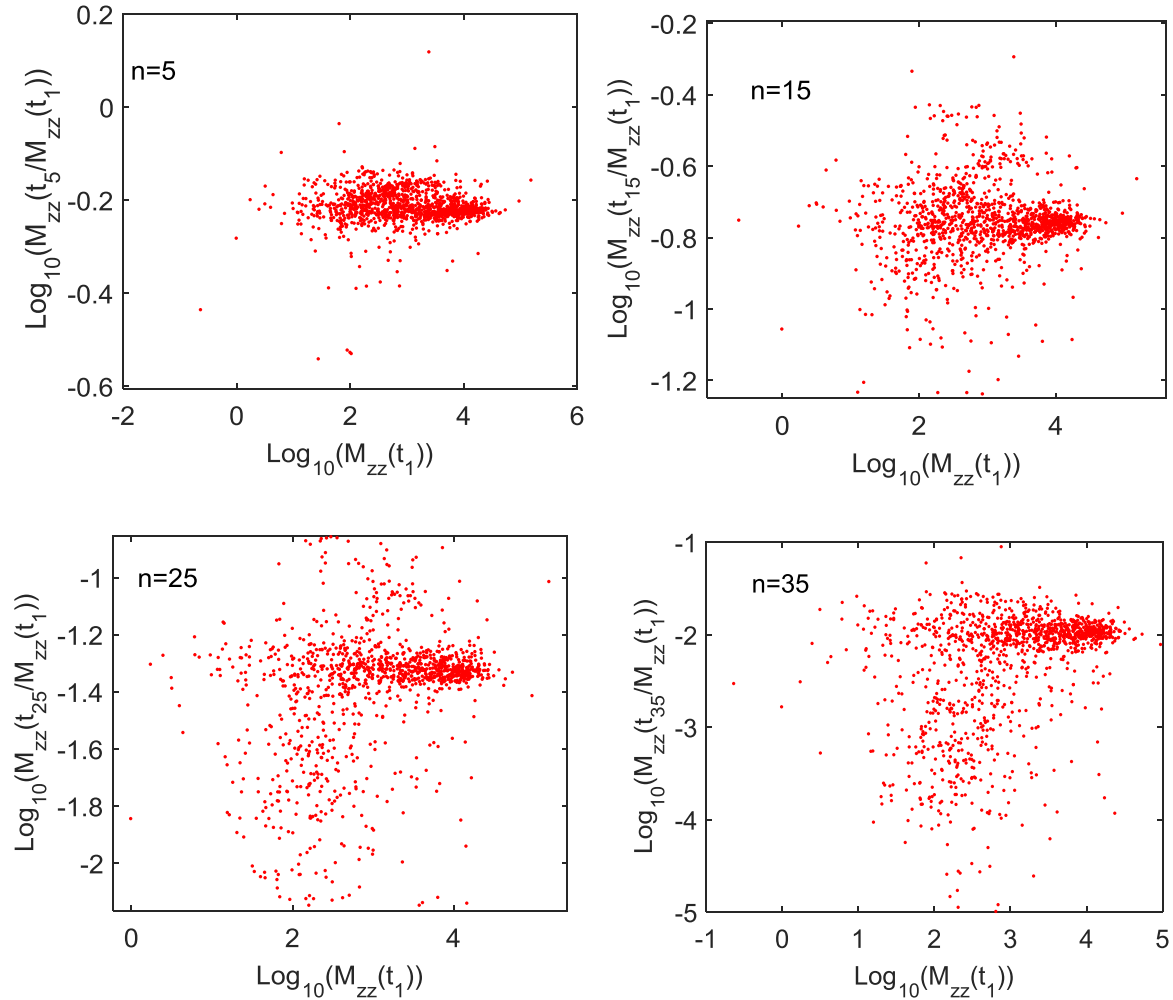
Figure 4. Scatter plot of size and decay for all WMA anomalies based on the extracted total ONVMS for time channels N# 5, 15, 25, and 35.

Step 5. Create a custom training list. We use the size i.e. magnitude of the inverted primary effective polarizability $M_{zz}(t_1)$ ($M_{zz}(t)$=(ONVMS$_{zz}$(t)) at the first time channel and decay i.e. ratio of the primary effective polarizability at the n-th time channel $M_{zz}(t_n)$ to that at the $M_{zz}(t_1)$ as classification feature parameters and determined the best separations. The values of $\log_{10}[M_{zz}(t_n)/M_{zz}(t_1)]$ versus $\log_{10}[M_{zz}(t_1)]$ are plotted for all WMA MM data sets, at the 5th, 15th, 25th, and 35th time channels. Visual examination shows that there are no distinguishable clusters at the 5th channel; at later times, on the other hand, the decay-vs.-size distribution starts to cluster. We used the features evaluated at the 35th time channel and applied statistical classification techniques [11], namely data were clustered using Euclidean distance and Ward linkage (for more info see [13]). For each cluster we computed the centroid and determined

the anomaly closest to it. We included this anomaly in the custom training data list. The clustering results of all WMA MM anomalies are depicted in Figure 5. Here each circle is centroid of a cluster and dots with the same color in and around the circle belongs to a cluster; In addition to the statistical clustering algorithm, ONVMS time decay curves were inspected for each anomaly: we used the TONVMS time decay shapes and symmetries to further validate or modify the custom training anomaly list. Anomalies with significantly asymmetric TONVMS were removed from the training list; anomalies with fast decay but symmetric profiles were added to the training list for which we requested the identifying ground truth.
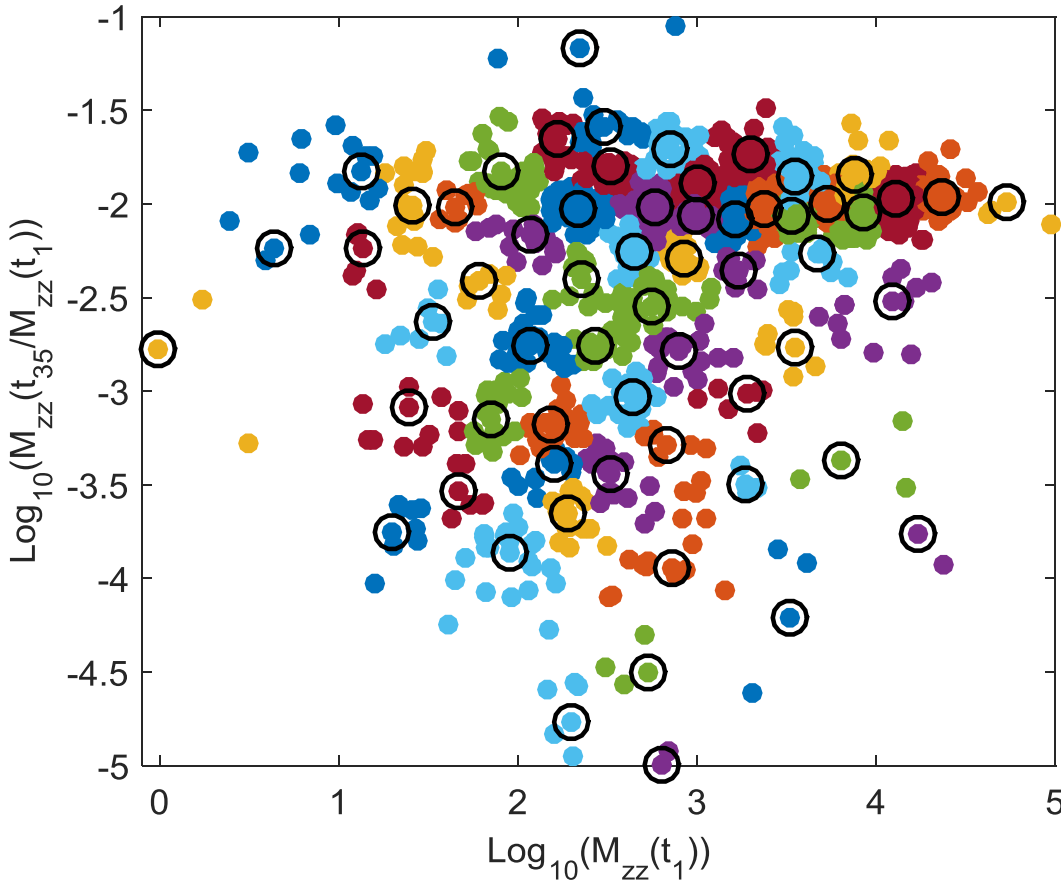
Figure 5. Result of the clustering for the WMA anomalies using the size and shape information for $n = 35$. The circles denote the anomalies for training.

Step 6. Request ground truth for selected anomalies. The custom training list, a combination of JD, clustering and ONVMS-DE single-target inversion results, was submitted to the ESTCP office, which then provided the ground truth for training. We used the delivered ground truth to identify the different possible TOI types and their size variations. There were seeded small and medium size ISO-s, 37 mm and 81 mm projectiles and 60 mm mortars which the ESTCP office identified as TOI.
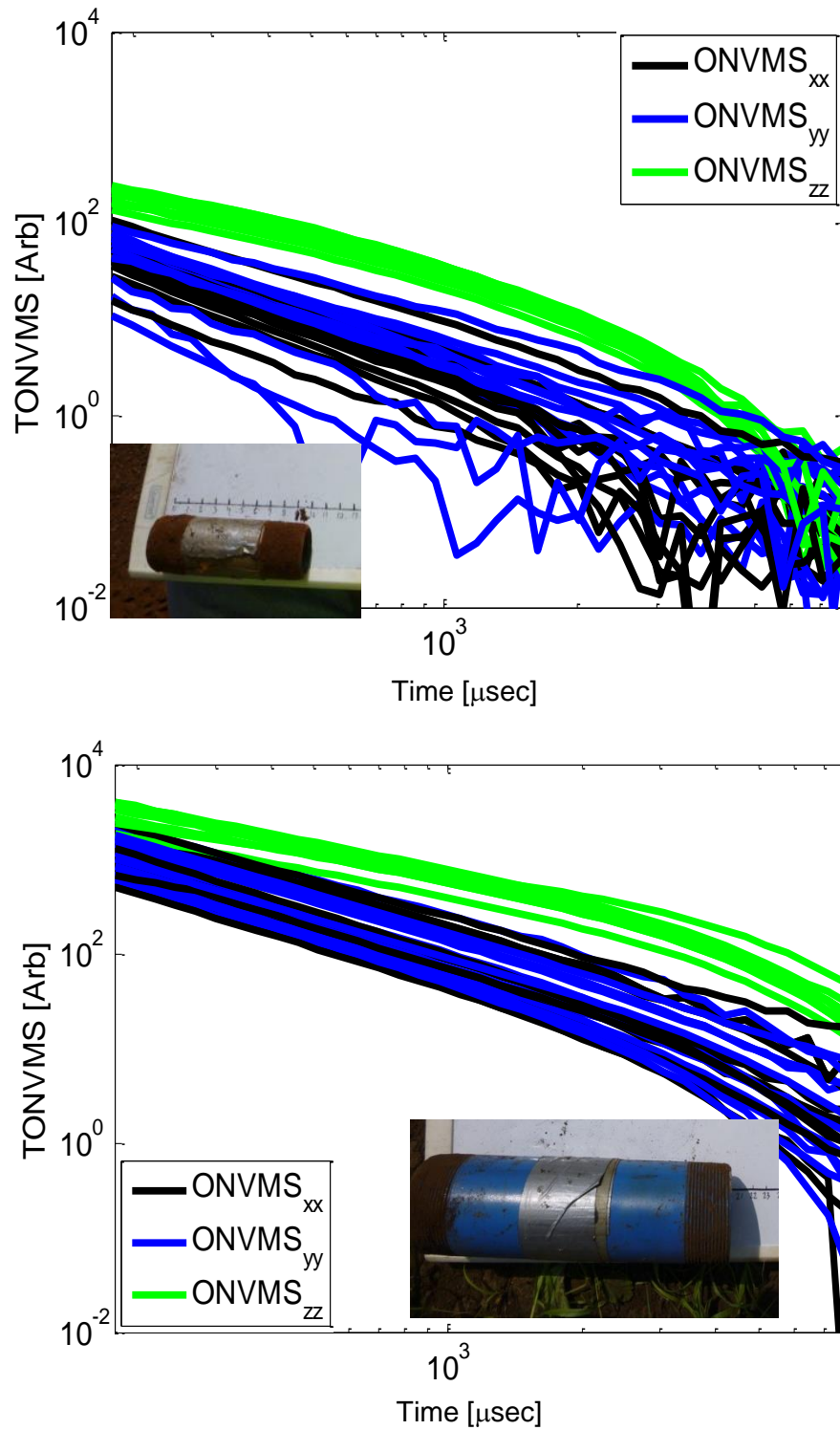
Figure 6. Inverted total ONVMS time-decay profiles for a small (top figure) and medium (bottom figure) WMA ISO targets.
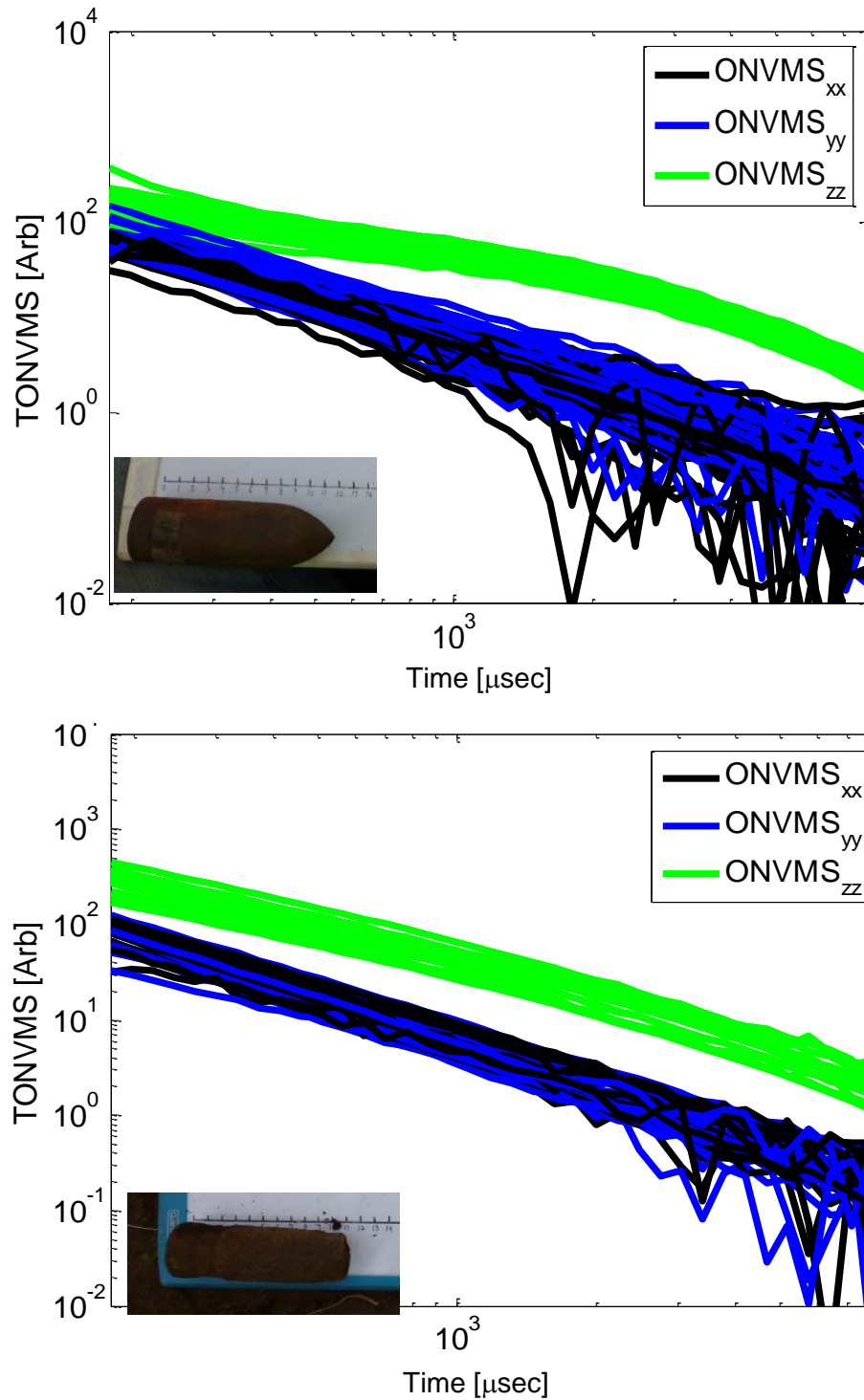
Figure 7. Inverted total ONVMS time-decay profiles for WMA 37 mm projectiles with (top figure) and without (bottom figure) copper band.
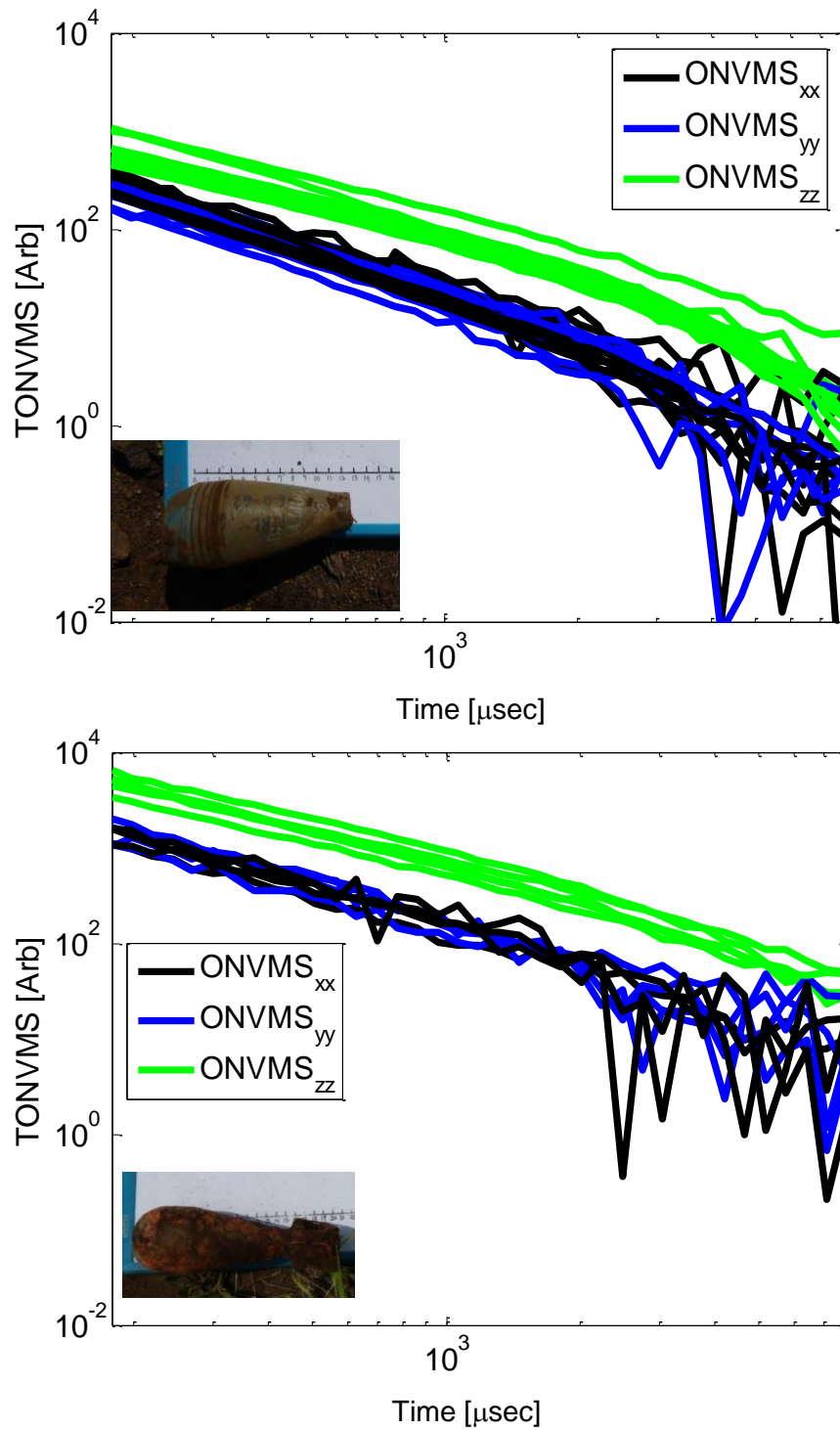
Figure 8. Inverted total ONVMS time-decay profiles for WMA 60 mm mortar without (top figure) and with (bottom figure) tail.
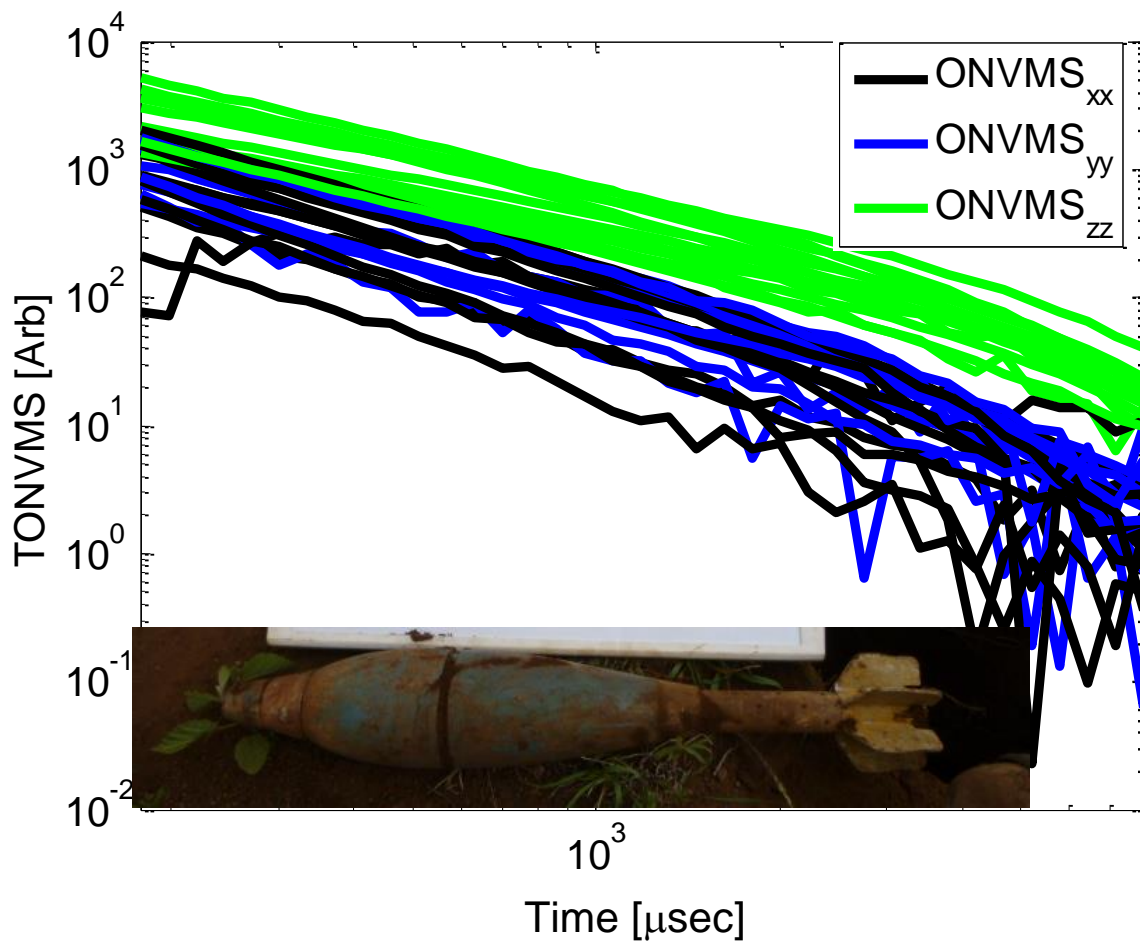
Figure 9. Inverted total ONVMS time-decay profiles for WMA 81 mm projectiles.

Step 7. Create ranked dig list. Armed with the ground truth of (a total of 87) custom identified training anomalies and the inverted total ONVMS for each MM cued data, we created a library for all TOI. The inverted total ONVMS for the anomalies that were classified as TOI appear in Figure 6-Figure 10. All the inverted total ONVMS are seen to cluster reasonable well, and each target has a total ONVMS with features that make it easy to identification: its amplitude at the first time channel, its decay rate, or the separation between the primary (green lines) and secondary (black and blue) components at different time channels. It is worth noting that the inverted total ONVMS for 37 mm projectiles are clustered more closely than for other TOI targets. To classify targets accurately, we used a classification approach based on symmetry and time-decay shapes, and ranked some of symmetric targets as TOIS.
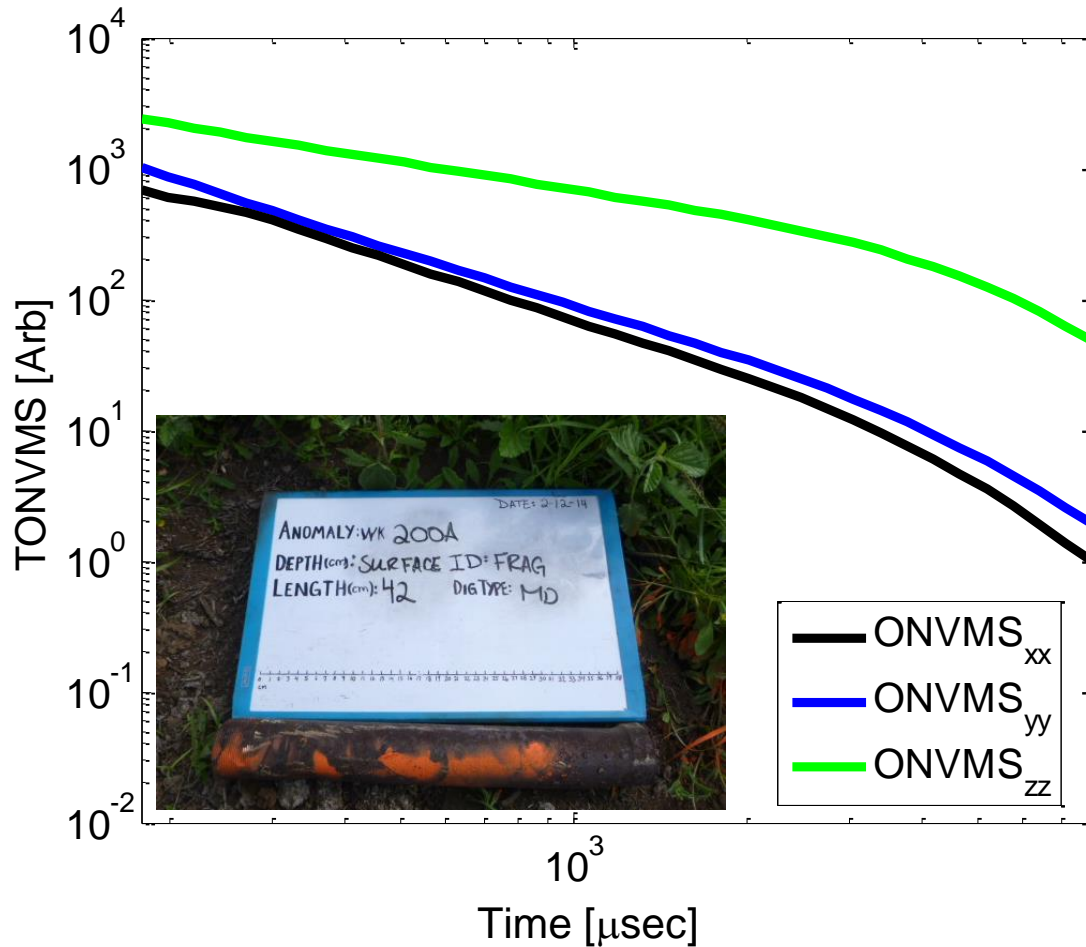
Figure 10. Inverted total ONVMS time-decay profiles for 2.36" rocket part, which was identified as TOI.

Step 8. Submit the dig list to ESTCP. The final prioritized dig list was submitted to the Institute for Defense Analyses (IDA) for independent scoring. The scored results were sent back in the form of a receiver operating characteristic (ROC) curve, which we depict in Figure 11. The result shows that of the 87 targets that were dug for training, 57 targets were not TOI (shift along *x*-axis) and 30 were (shift along *y*-axis); all TOI targets were ranked as dig except one small ISO and one 60 mm mortar, which laterally were offset more or about than 30 cm from the center of MM sensor. The result clearly shows that advanced EMI sensing and classification technologies can be applied to active and challenge UXO sites, which in addition to man-made clutter also consist magnetic soils. Our studies show that even when targets are buried in a highly susceptible magnetic soil, the technology provides

the ability to leave at least 80% of clutter items in the ground if the lateral offset between the sensor's center and acquired target is less than 30 cm.
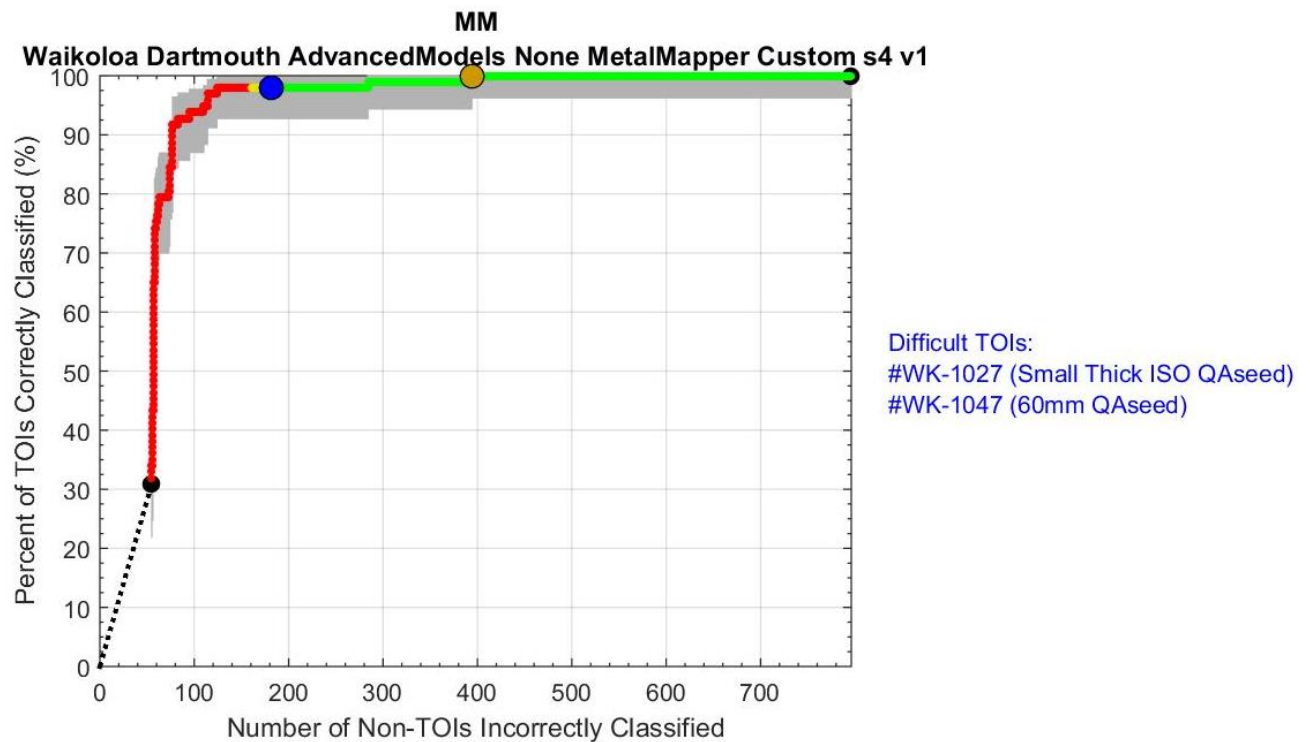
Figure 11. ROC curve for the WMA, HI MM data.

3.2 A Brief Chronological Summary

The basic concepts of the Advanced EMI models have evolved largely from methodologies developed over the last eleven years by the Electromagnetic Sensing Group at Dartmouth College in close collaboration with the ERDC-CRREL team. The developments were supported by various SERDP projects. In 2007, SERDP awarded Project MM-1572, "A Complex Approach to UXO Discrimination: Combining Advanced EMI Forward and Statistical Signal Processing" to Sky Research, Inc. This project supported the development and implementation of NSMS, an advanced and physically complete EMI model, and its combination and integration with statistical classification algorithms such as neural networks, support vector machines, and Gaussian mixture model clustering. These methods were tested at the APG, Camp Sibert, and SLO live sites. The NSMS method was extended into the orthonormalized volume magnetic source (ONVMS) technique. The basics of the ONVMS/Joint Diagonalization technique were developed under the following SERDP projects: "Electromagnetic Induction Modeling for UXO Detection and Discrimination Underwater/Multi Target Inversion and Discrimination" (MM-1632, Dartmouth College) and "Isolating and Discriminating Overlapping Signatures in Cluttered Environments" (MM-1664, a joint project between Dartmouth College and USACE-CRREL). The ONVMS and JD approaches were tested at Camp Butner and Camp Beale under Projects SERDP MR-1572 and ESTCP MR-201101, respectively.

4.0 PERFORMANCE OBJECTIVES

The performance objectives of this ESTCP live-site discrimination study are to achieve high probability of discrimination of UXO from a wide range of clutter items, to process all data sets, to minimize number of Can't analyze/Can't decide targets, to minimize number of false positives, and to identify all UXO with high confidence. The performance objectives are summarized in

Table 1.

Table 1. Performance Objectives

Performance Objective	Metric	Data Required	Success Criteria
Maximize correct classification of munitions	Number of targets-of-interest retained	• Prioritized anomaly lists • Scoring reports from Institute for Defense Analyses (IDA)	Approach correctly classifies all targets-of-interest
Maximize correct classification of non-munitions	Number of false alarms eliminated	• Prioritized anomaly lists • Scoring reports from IDA	Reduction of false alarms by >75% while retaining all targets of interest
Specification of no-dig threshold	Probability of correct classification and number of false alarms at demonstrator operating point	• Demonstrator-specified threshold • Scoring reports from IDA	Threshold specified by the demonstrator to achieve the above criteria
Minimize number of anomalies that cannot be analyzed	Number of anomalies that must be classified as "Unable to Analyze"	• Demonstrator target parameters	Reliable target parameters can be estimated for > 90% of anomalies on each sensor's detection list
Correct estimation of target parameters	Accuracy of estimated target parameters	• Demonstrator target parameters • Results of intrusive investigation	Total ONVMS ± 10% X, Y < 10 cm Z < 5 cm size ± 10%

4.1 Objective: maximize correct classification of munitions

The effectiveness goal of the technology for discrimination of munitions is maximizing correct classification of targets of interest vs. non-TOI with high (95%) confidence. The confidence interval is calculated from a partial (up to dig stop point) ROC.

4.1.1 Metric

Identify all seeded and native TOI with high confidence using advanced EMI discrimination technologies. Our estimates were based on using the extracted total ONVMS as input to statistical and template matching algorithms.

4.1.2 Data requirements

We analyzed MM data and identified custom training data sets (using less than <5 % of entire data). We requested the ground truth for the custom training data sets and used them to validate the models. We generated a dig list that was scored by IDA.

4.1.3 Success criteria evaluation and results

The objective was considered to be met if all seeded and native UXO items could be identified below an analyst-specified no-dig threshold.

4.1.4 Results

Our algorithm was able to classify all TOI-s correctly, but two TOIs: one small ISO and one 60 mm mortar. Figure 11 shows the ROC curves obtained for all WMA anomalies.

4.1.5 Root cause analysis

To understand the cause of miss-classifying these two TOIs we re-examined classification procedures for all WMA anomalies. Classification studies were conducted at three T017 and T20-A and T020-B areas. These T017 and T020 areas were chosen to understand how lava flows under them effect on geological background responses and targets classifications. The T017 site is near the coast and the lava flow underlying it is considerable younger, than the lava flow underlying the two T020 sites. The both missed TOIS were in area T017. To assess geological background responses, we analyzed largest eigenvalues versus time for soils in these areas when the sensor is placed on the ground. The results in Figure 12 show that geological background response for the T017 area is higher than background responses for area T020A and T020B. Usually high background responses degrade data and causes miss-classifications, particularly when targets lateral offsets are more or about 30 cm from the center of the sensor.
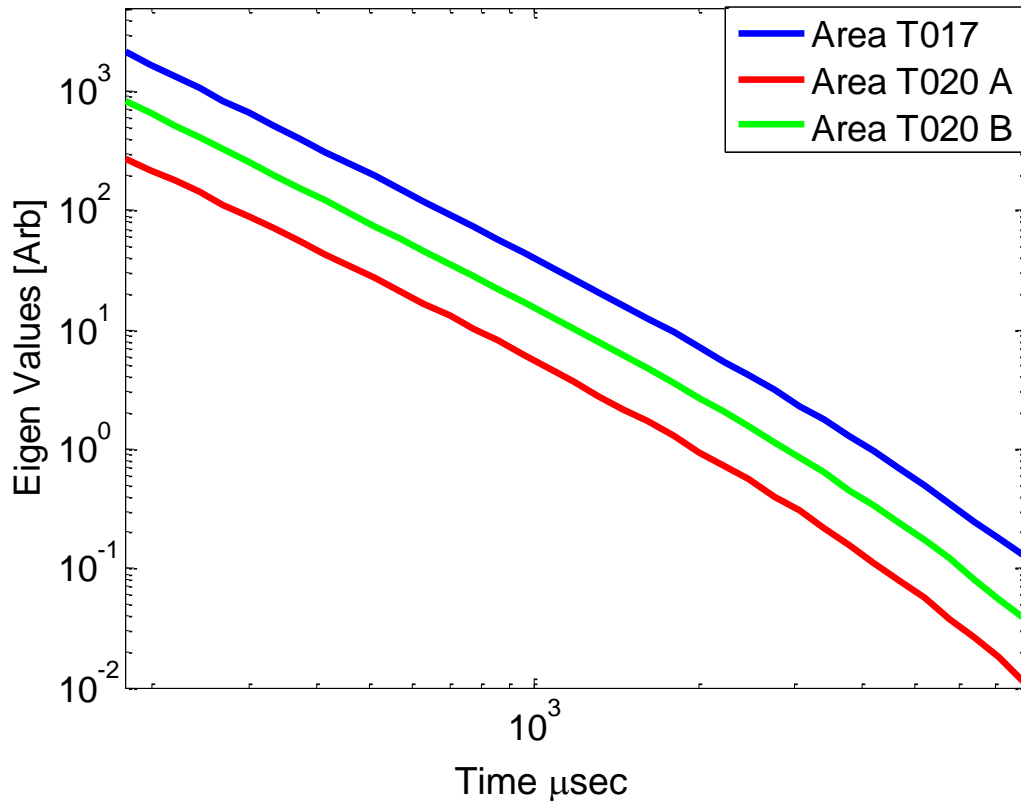
Figure 12. Eigen values vs time for three T017, T020 A and T020B areas.

In addition to geological background noises, a sensor's malfunction significantly effects on targets classification as well, particularly when the failed sensor is close to the targets. Unfortunately, during the WMA MM data collection one of the receivers failed completely. Namely, all three components of Rx #0 did not work properly, and fields measured by the Rx #0 were not included in data inversion and processing. The inverted total ONVMS (effective polarizabilities) and eigenvalues for the miss-classified small ISO (anomaly #1027) and 60 mm mortar (anomaly# 1047) are depicted on Figure 13. The inverted effective polarizabilities for the anomaly #1027 shows some symmetry but its magnitude is much smaller than for a library ISO target, see Figure 6. Also, eigenvalues versus time shows that there is a significant soil response (eigenvalues linear decay in log-log plot, see Figure 12) as well. To better understand why the inverted effective polarizabilities for anomaly #1027 do not match the effective polarizabilities for a library small ISO target, we checked the distance between the MM sensor's center and dug target location. The analysis show that for the anomaly #1027, the sensor's center was located 28 cm from the target. Since this offset is less than 30 cm, the extracted classification parameters should have been robust and closely correlated with the effective polarizabilities for a library small ISO-s target. However, after further investigation it was found that the closest Rx sensor to the target was the failed Rx #0 sensor. This and the dominant ground responses in other sensors cause the algorithm to miss-classify this small target. We believe, that positioning the center of the sensor closer to the

anomaly, or having properly working Rx adjacent to the target could have avoided this misclassification.

For seed WK-1047, the sensor was located 43 cm from the target. This offset is significantly outside the 30 cm objective radius and, as a result the extracted polarizabilities values are high but not symmetric, decay linearly in log-log scale and looks like more a soil's characteristic, then signals from a compact 60 mm mortar target. While in case of non-permeable soil conditions, our algorithms were able to obtain accurate classification features at more than 30 cm offsets, we believe the presence of a significant magnetic ground response made it very difficult to extract robust classification features with the sensor at this 43 cm location for anomaly #1047.
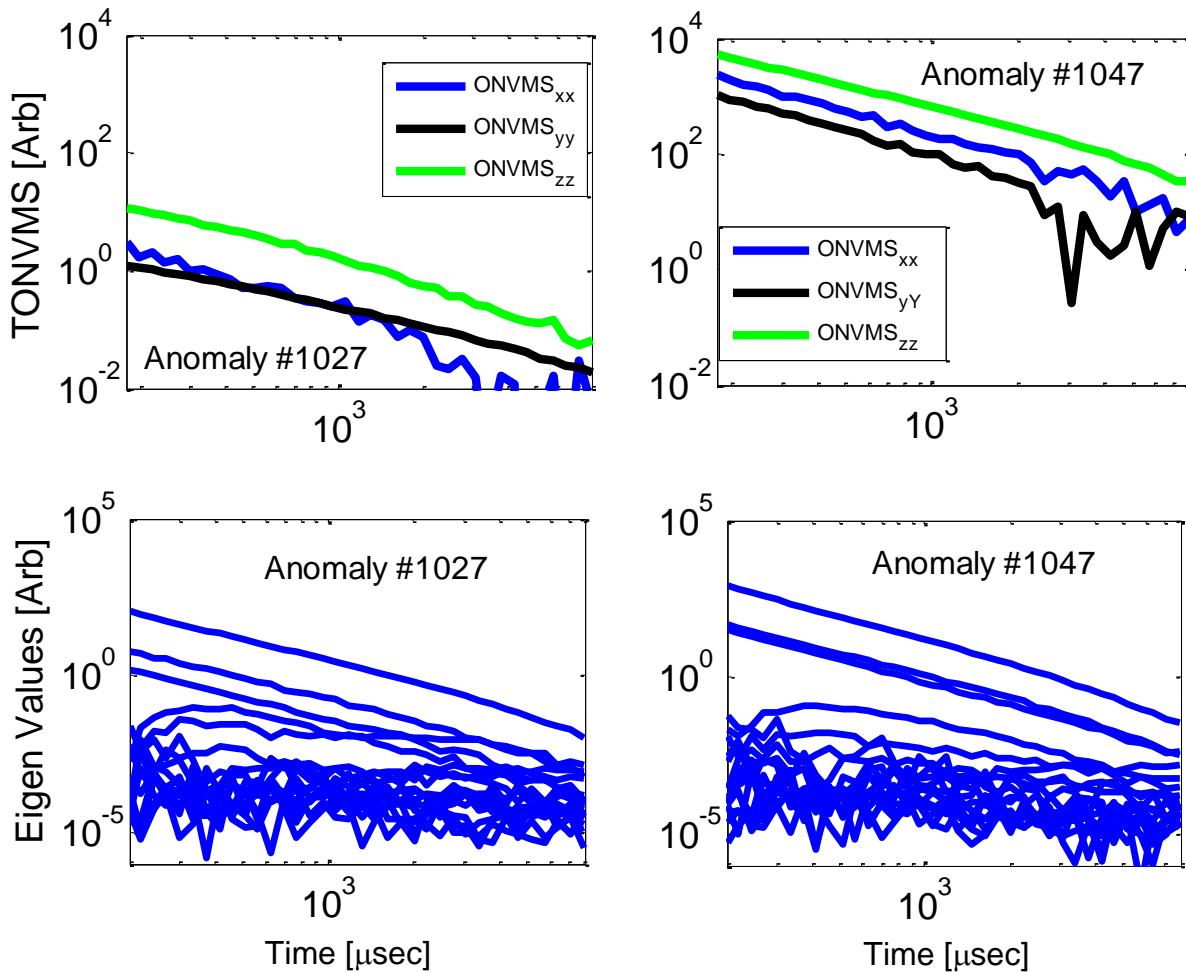
Figure 13. Total ONVMS and eigenvalues for missed small ISO (anomaly #1027) and 60 mm mortar (anomaly #1047) targets;

Figure 14. Photos of intrusive investigated anomalies #29, #36, #199, #441, #442.

4.1.6   Mystery targets: discrepancies between classification and intrusive results

All intrusive operations at WMA site were conducted by Parsons's Personnel. According to the report MR-201104-DR-Waikoloa [30]: Parsons used the Minelab Explorer SE to determine the initial approach to every target and as a screening process to assess if metal was present in the subsurface or if the anomaly was caused by the local geology. If the Minelab Explorer SE
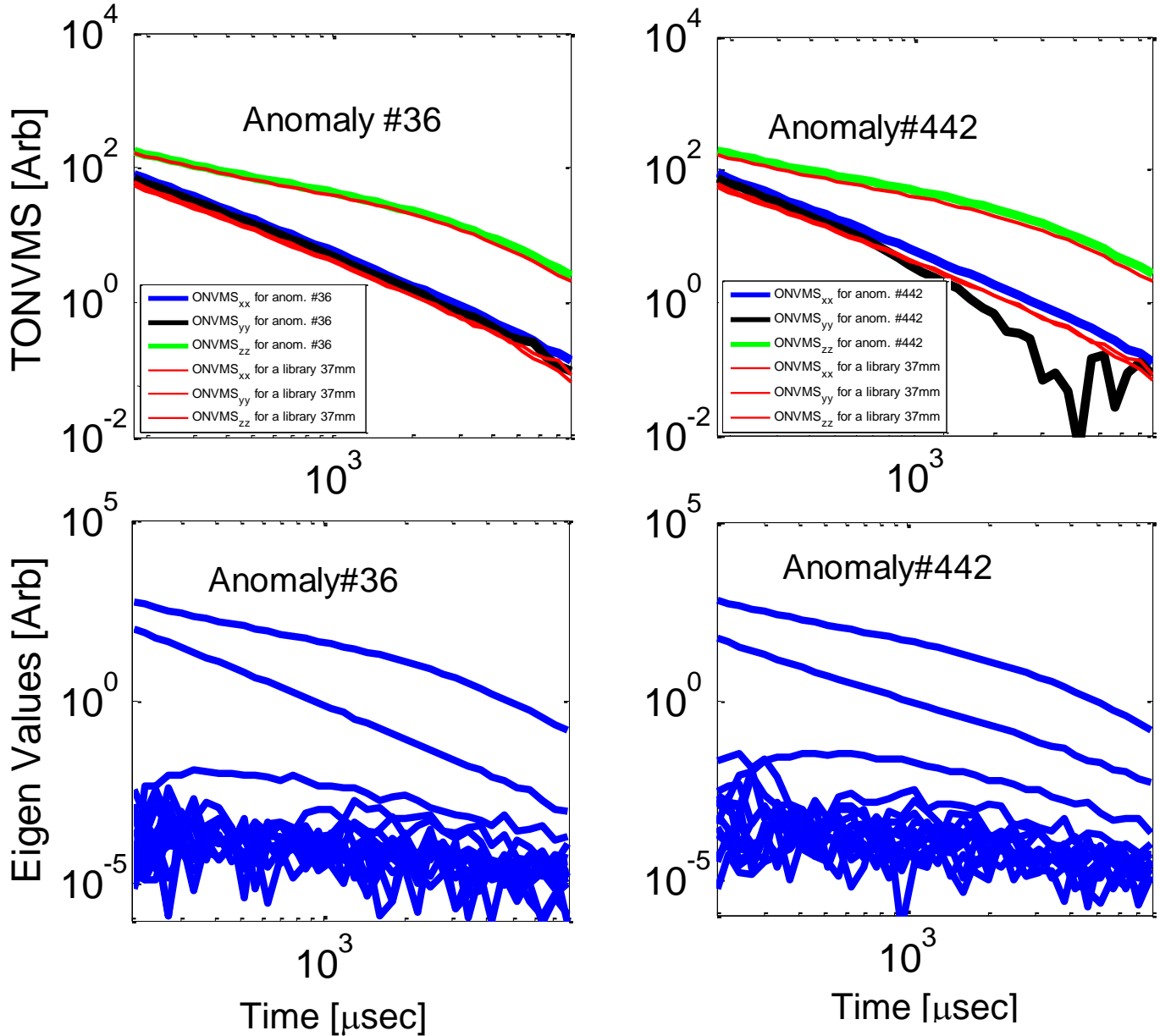
Figure 15. Top row: comparisons between total ONVMS for a library 37 mm projectile (red lines), with copper band, and for anomalies #36 and #442. Bottom row eigenvalues versus time for anomalies #36 and #442.

indicated that there was no metal present in the area, the anomaly was considered a "no contact." A GPS point was then taken at the location of the flag and a photograph was collected of the area surrounding the flag. If the Minelab Explorer SE indicated that there was metal present in the subsurface, then the UXO technicians excavated the item. Location data captured by GPS were used to document the center mass and depth of each item. A photograph was collected of the item; Lastly, an EM61 unit was used to scan the location to confirm the absence of all metallic items from that target location or that the pre-millivolt reading had been reduced by at least 75%.
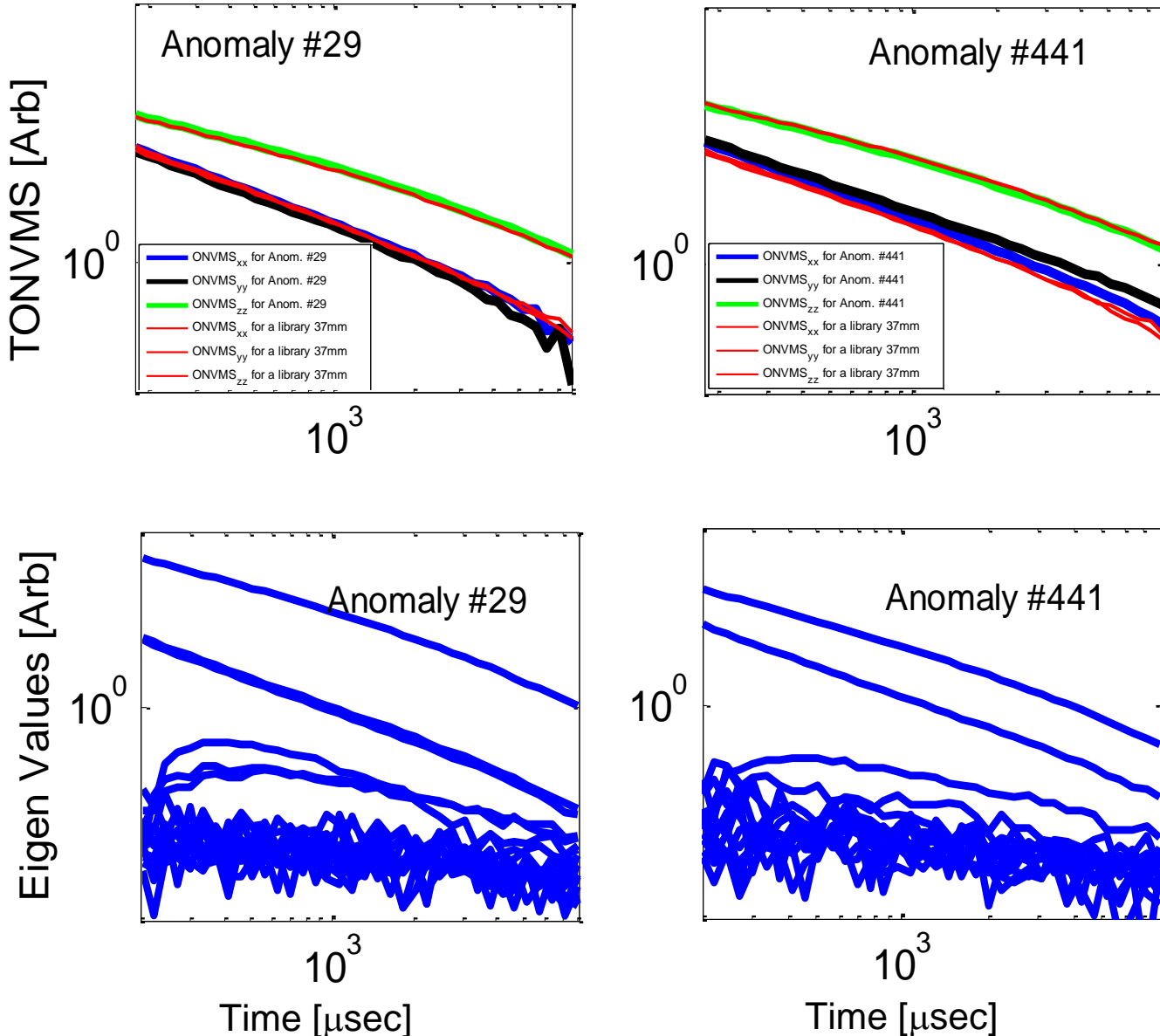
Figure 16. Top row: comparisons between total ONVMS for a library 37 mm projectile (red lines), without copper band, and for anomalies #29 and #441. Bottom row eigenvalues versus time for anomalies #29 and #441.
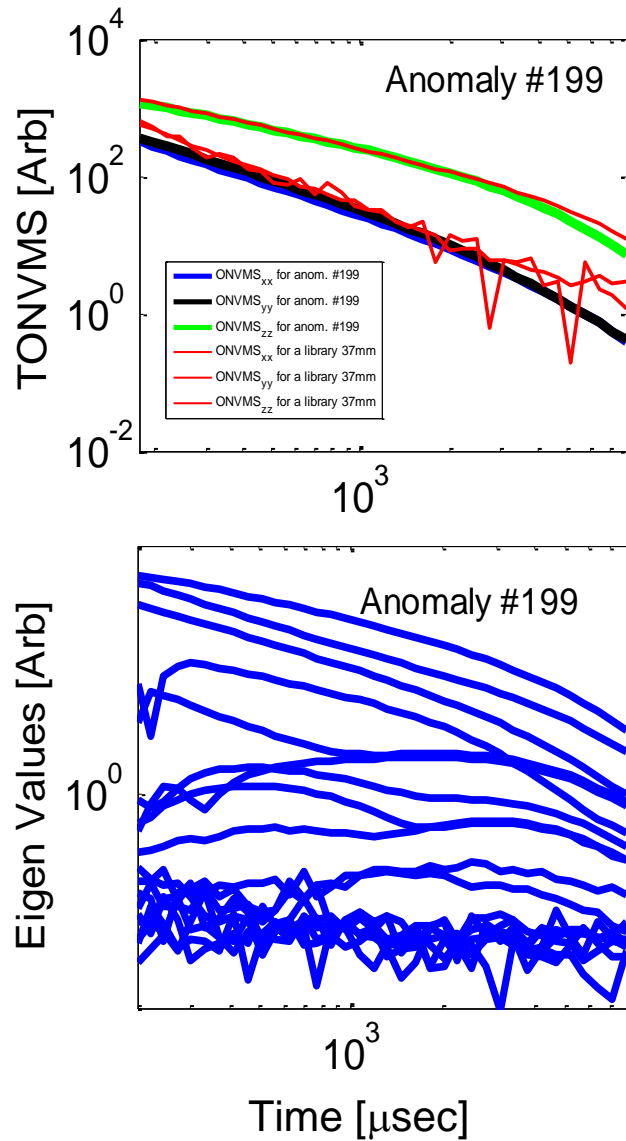
Figure 17. Top row: comparisons between total ONVMS for a library 60 mm projectile (red lines and for anomaly #199. Bottom row eigenvalues versus time for anomaly #199.

Using the above described intrusive investigation approach, Parsons considered anomalies #29, 36, 199, 441, and 442 as "no contacts" see Figure 14. However, MM data and our classification results depicted in Figure 15, Figure 16 and Figure 17 clearly show that there are compact metallic targets (see eigenvalues vs time and total ONVMS). The effective polarizabilities of these anomalies closely match the polarizabilities of library 37 mm projectiles and 60 mm mortar, indicating that the intrusive procedure failed to document all detected targets correctly, or failed detect and clear all hazardous targets on the site. If later occurred, then we believe that the MineLab explorer SE is not a suitable system for metallic targets detection in magnetic soil, and for accurate cleaning UXO sites the classification results must be used to guide and validate intrusive investigation results.

4.2 Objective: maximize correct classification of non-munitions

The technology aims to minimize the number of false negatives, i.e. maximize the correct classification of non-TOI.

4.2.1 Metric

We compared the number of non-TOI targets that can be left in ground with high confidence using the advanced EMI discrimination technology to the total number of false targets that would be present if the technology were absent.

4.2.2 Data requirements

This objective requires the prioritized anomaly list, which was created by our team, and independent scoring reports from IDA.

4.2.3 Success criteria evaluation and results

The objective was considered to have been met if the method eliminated at least 75% of targets that did not correspond to targets of interest in the discrimination step.

4.2.4 Results

Due to high background noise, the sensor's large lateral offset from anomalies and failure of one of the sensors, this objective was not met successfully. The advanced EMI discrimination technology was able to eliminate 50% of non-TOI in the WMA demonstration after all TOI were classified correctly.

4.3 Objective: specify a no-dig threshold

This project aims to provide high classification confidence approach for UXO-site managers. One of the critical quantities for minimizing UXO residual risk and providing regulators with acceptable confidence is the specification of a no-dig threshold.

4.3.1 Metric

We compared an analyst's no-dig threshold point to the point where 100% of munitions were correctly identified.

4.3.2 Data requirements

To meet this requirement, we needed scoring reports from IDA.

4.3.3 Success criteria evaluation and results

The objective would be met if a sensor-specific dig list placed all the TOI before the no-dig point and if additional digs (false positives) were requested after all TOI were identified correctly.

4.3.4 Results

This objective was not met. All TOI-s, except two, were located before the analyst's no-dig threshold point see Figure 11.

4.4 Objective: minimize the number of anomalies that cannot be analyzed

Some anomalies may not be classified, either because of the data are not sufficiently informative—the sensor physically cannot provide the data to support classification for a given target at a given depth—or because the data processing was inadequate. The former is a measure of instrument performance for all anomalies for which all data analysts converge. The latter is a measure of our data analysis quality, where our target diagnostic differs from that made by other analysts.

4.4.1 Metric

The metric for this objective is the number of anomalies that cannot be analyzed by our method, and the intersection of all anomaly lists among all analysts.

4.4.2 Data requirements

Each analyst submitted their anomaly list. IDA scored all lists and returned a list of anomalies that could not be analyzed by any analyst ("cannot analyze" or "failed classification").

4.4.3 Success criteria evaluation and results

The objective was met if at least 95% of the selected anomalies that verify the aforementioned depth requirement could be analyzed.

4.4.4 Results

This objective was successfully met. All data sets for all anomalies, except one, were analyzed. Only one anomaly, which did not have appropriate data, was ranked as "cannot analyze."

4.5 Objective: correct estimation of target parameters

The combined ONVMS-DE algorithm provides intrinsic and extrinsic parameters for the different targets. The intrinsic parameters were used for classification, while the extrinsic parameters (i.e., target locations) were utilized for residual risk assessment.

4.5.1 Metric

The classification results entirely depend on how accurately these parameters are estimated.

4.5.2 Data requirements

To achieve this objective, we inverted and tabulated the intrinsic and extrinsic parameters for all targets. To validate the extracted extrinsic parameters, we needed the results of intrusive investigations.

4.5.3 Success criteria evaluation and results

The objective was met if the targets' intrinsic parameters varied within ±10%, the extracted *x-y* location within ±10 cm, and the depth within ±5 cm.

4.5.4 Results

Figure **18** and Figure 19 show the distribution of depth (defined here by as $C_{data} - C_{estimated}$) where C= X, Y, and Depth) and lateral positions errors respectively. The estimated and measured depths discrepancies for TOI targets have a mean of 1.6cm and a standard deviation of 5 cm, and lateral position errors along *x* and *y* directions have means 0.25 cm and 4.8 cm standard deviations 10 cm and 7.5 cm, respectively. Thus overall the agreement between inverted and actual values of depth and lateral positions were acceptable, however, Figure **18** and Figure 19 show that estimated depth and locations were outside the required criteria specified in the table 1. We believe that these could be related to surface roughness and topology, recording accuracies of extrinsic parameters and recovered targets in the cell.
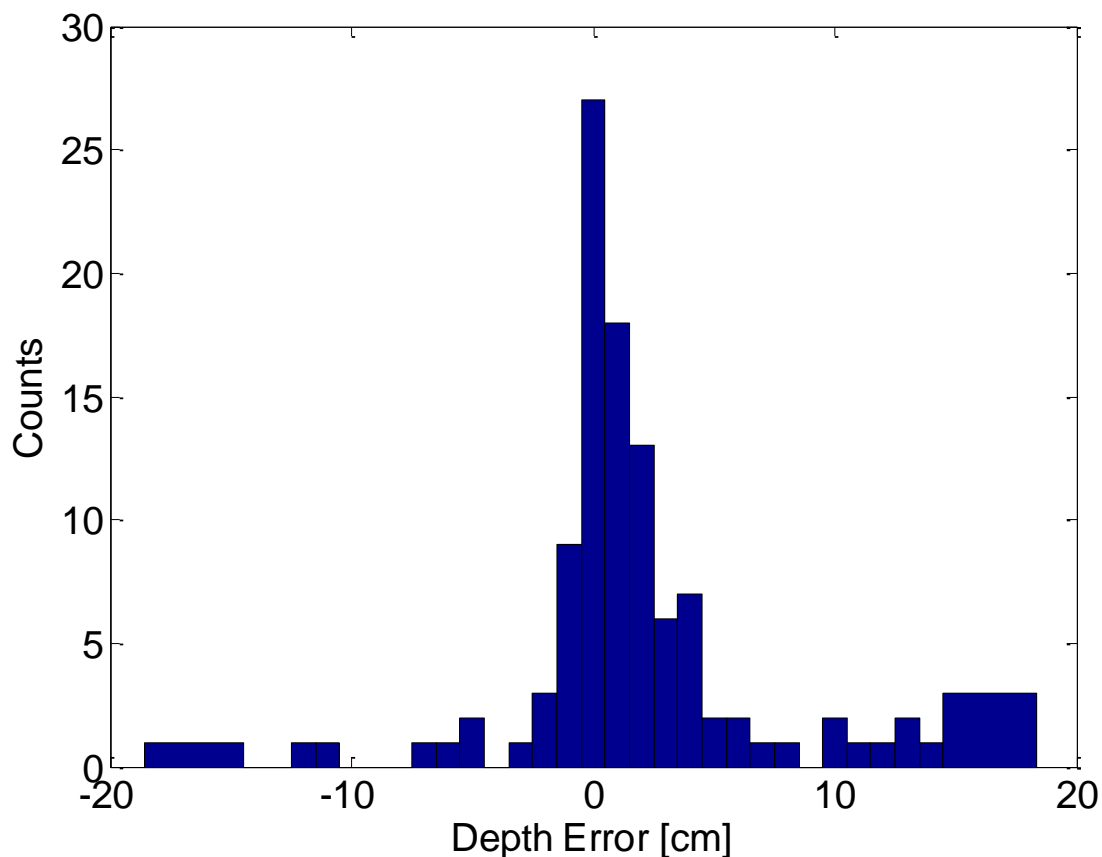
Figure 18. Histogram of depth errors (defined as ($Z_{estimated}$-Z_{data})) for the WMA TOI anomalies. The distribution shown has a mean of 1.6 cm and a standard deviation of 5 cm. There is good agreement between the estimates and the ground truth.
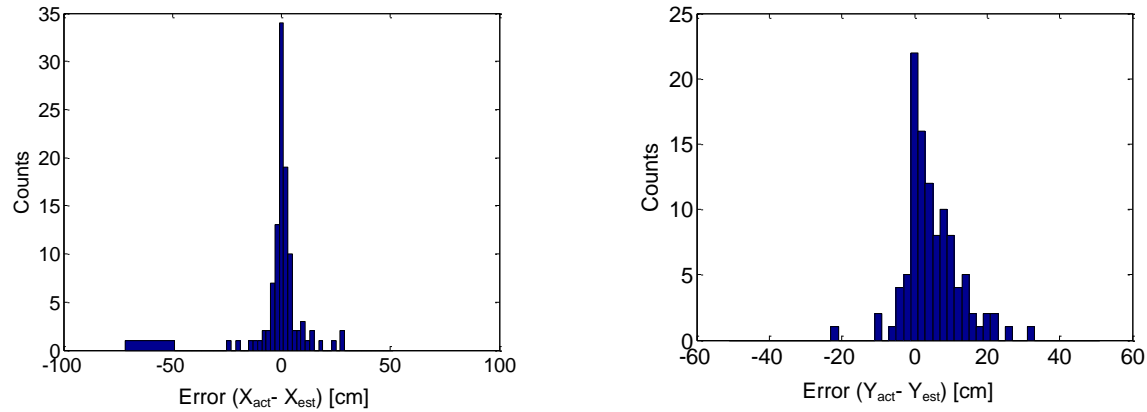
Figure 19. Histogram of lateral (*x*,*y*) errors (defined as (left) $X_{measured}$– $X_{estimated}$ and (right) $Y_{measured}$– $Y_{estimated}$) for the WMA TOI targets. Lateral errors in x and y directions have means 0.25 cm and 4.8 cm and standard deviations 10 cm and 7.5 cm, respectively.

5.0 TEST DESIGN

The only required test at the WMA site entailed collecting target characterization training data: Using a calibration pit, the data-collection team made a series of static measurements of example targets at several depths and altitudes in order to cross-check models, confirm Tx and Rx polarity for the sensors, and characterize the so-called Library targets.

5.1 Demonstration Schedule

Table 2: Demonstration steps

Tasks and demonstration stages	Preparation calibration	Blind data set		Post-survey analysis
	Feb 2015	Mar-2015	May-2015	December-2015
1. Invert all calibration data sets	X			
2. Invert MM data sets		X		
3. Build custom training data sets and request ground truth for MM		X		
4. Redefine MM target classifier and request additional training data if necessary			X	
5. Generate final dig list and submit to IDA			X	
6. Conduct retrospective analysis if needed				X
REPORTING:				
7. Draft demo plan	X			
8. Final demo plan	X			
9. Draft demonstration report				X
10. Final demonstration report				X

Figure 20. Gantt chart showing schedule of detail activities to be conducted during the WMA ESTCP MM data inversion and classification study.

6.0 DATA ANALYSIS PLAN

We analyzed all cued data for the MM sensor and produced prioritized dig lists for independent scoring.

6.1 Extracting Target Locations

Target locations were determined relative to the sensor coordinate system using the differential evolution algorithm. Object responses were modeled with ONVMS. The combined ONVMS-DE algorithm was run for single- and multi-target cases and provided target locations.

6.2 Extracting Target Intrinsic Parameters

6.2.1 Single targets

The combined ONVMS-DE algorithm yields the targets' intrinsic total ONVMS, which we used for classification. The total ONVMS contains three moments, $M_{xx}(t)$, $M_{yy}(t)$, and $M_{zz}(t)$, along the primary axes in the target's own reference frame. These moments are similar to simple dipole moment components but carry more information, accounting for the targets' inherent heterogeneities. The ONVMS-DE algorithm outputs the time-decay curves of the target's total ONVMS tensor $M_{ij}(t_k)$. The next step is to determine the time decay of the primary components of the total ONVMS in the target's reference frame. While this can be done by standard diagonalization—i.e., finding $M(t_k) = V(t_k)D(t_k)V^T(t_k)$, where $V(t_k)$ contains the eigenvectors of $M(t_k)$—it is more convenient to perform a joint diagonalization,

$M(t_k) = VD(t_k)V^T$, where now the eigenvectors are shared by all time channels; this allows us to extract more reliable total ONVMS values and reduce uncertainty. The resulting temporal decay of the total principal ONVMS for the MM anomalies are illustrated in **Figure 6**-Figure 10.

6.2.2 Multi-target cases

A similar approach is carried out if more than one subsurface target is expected. The DE algorithm now searches for the locations and the total ONVMS of several objects. Such multi-target inversion is crucial in the field for cases in which a signal from a UXO is mixed with EMI signals from nearby clutter. Our two-target inversion code yields three sets of location and total ONVMS estimates: one for Target 1, one for Target 2, and a combined estimate with Targets 1 and 2 represented by a single object. (In the case of 3-target inversion, seven sets of data are expected: only Target 1, only Target 2, only Target 3, Targets 1 and 2 as a single object, Targets 2 and 3 as a single object, Targets 1 and 3 as a single object, and all three targets acting as a single object. In the general case of *n* targets one expects *n* (*n* – 1) + 1 sets of ONVMS curves).

6.3 Selection of Intrinsic Parameters for Classification

Most UXO are bodies of revolution, and thus the two secondary polarizability elements are degenerate. However, live-site UXO discrimination studies have repeatedly shown that this

symmetry can be compromised due to low SNR, especially for small or deep targets. A good classification of object features can then be obtained by using only the principal component of the total ONVMS (M_{zz}). Furthermore, to limit the number of relevant features for use in classification we extract parameters exclusively from the main polarizability $M_{zz}(t)$, both to represent size $M_{zz}(t_1)$ and wall thickness $M_{zz}(t_n)/M_{zz}(t_1)$.

6.4   Training

Our classification approach is based on custom training data. At the first stage of the process we used a semi-supervised clustering technique for identifying potential site-specific TOI. Below are the basic steps performed during training data selection; for more details regarding each specific sensor see Section 2.3.

(a) The targets' intrinsic features ($M_{zz}(t_1)$, $M_{zz}(t_n)/M_{zz}(t_1)$) were selected from the extracted total ONVMS; *n* was chosen based on feature separation. EMI data sets of all anomalies, corresponding to single-and multi-object inversions, were produced.
(b) Initial clustering was performed. The ground truth was requested for all targets whose features were located closest to the corresponding cluster centroid and had TOI-like ONVMS features.
(c) Clusters containing at least one TOI were identified, and a smaller domain was selected within the feature space for further interrogation.
(d) Additional clustering was performed within the selected domain, and those targets with features closest to the corresponding cluster centroids were probed for ground truth. The clusters with at least one identified UXO were marked as *suspicious*. The total ONVMS curves were inspected within the selected domain.
(e) All targets whose features (based on multi-object inversion and library matching) fell inside any of the *suspicious* clusters were used to train the statistical classifier and the library-matching procedure.

6.5   Classification

(f) Probability density functions were created for single- and multi-target scenarios.
(g) All of the unknown targets were scored based on the probability density functions.
(h) Dig lists were produced for both single-and multi-object cases and compared to each other to find similarities and differences.
(i) All items were further analyzed using library matching, and all total ONVMS time-decay curves were inspected visually.
(j) A set of anomalies were identified and additional training data sets were requested. The new information was incorporated into the Gaussian mixture model and all items were re-scored.
(k) Based on the previous steps, a classification threshold was selected and a final dig list produced.

6.6   Decision Memo

The algorithms used to select training data and to perform inversion and classifications for the WMA test are described in Section 2. Using the inversion, clustering, classification and data-requesting procedures outlined above, we produced a ranked anomaly list formatted as specified by IDA [20].

7.0 COST ASSESSMENT

Time and resources were tracked for each task to assess the cost of deploying the technology at future live sites. Note that some of the costs might decrease as the technology matures and survey procedures get formalized. A time and cost model of the resources spent during WMA target classification using the advanced models is summarized in Table 3. These estimations are done for a geophysicist with salary of $90/hr.

Table 3: Cost model for advanced EMI model demonstration at the WMA.

Cost Category	Description	Time	Cost
Preprocessing	Time required to perform eigenvalue extraction, check data quality, and estimate the number of potential anomalies	0.25 min/anomaly	$0.375/Anomaly
Parameter extraction	Time required to run code and extract target feature parameters	0.25 min/anomaly	$0.375/Anomaly
Classifier training	Time required to optimize classifier design and train	0.5 min/anomaly	$0.75 /Anomaly
Classification and construction of a ranked anomaly list	Time required to classify anomalies in the test set and construct the ranked anomaly list	1.0 min/anomaly	$1.5/anomaly
Reporting	Time required to generating and documenting classification results and writing reports.	2.0 min/anomaly	$3.0/anomaly
	Total	4 min/anomaly	$6/anomaly

8.0 MANAGEMENT AND STAFFING

Fridon Shubitidze – Principal Investigator. Responsible for MM data JD analysis, classification quality check and reporting.

Irma Shamatava – White River Technologies. Responsible for data inversion using the combined ONVMS/DE algorithm and classification.

.

9.0 REFERENCES

[1] F. Shubitidze, J. P. Fernández, B.E. Barrowes, I. Shamatava, A. Bijamov, K. O'Neill, D. Karkashadze, "The orthonormalized volume magnetic source model for discrimination of unexploded ordnance," *IEEE Transactions on Geo-Science and Remote Sensing, Digital Object Identifier 10.1109/TGRS.2013.2283346.*

[2] Shubitidze, F., et al., *Joint diagonalization applied to the detection and discrimination of unexploded ordnance.* Geophysics, 2012. **77**(4): p. Wb149-Wb160.

[3] R. Storn, and K. Price, "Differential evolution: a simple and efficient adaptive scheme for global optimization overcontinuous spaces," *Journal of Global Optimization*, vol. 11, pp. 341–359, 1997.

[4] R. Storn, "System design by constant adaptation and differential evolution," *IEEE Trans. Evol. Comput.,* vol. 3, pp. 22–34, 1999.

[5] F. Shubitidze, K. O'Neill, B. E. Barrowes, I. Shamatava, J. P. Fernández, K. Sun, and K. D. Paulsen, "Application of the normalized surface magnetic charge model to UXO discrimination in cases with overlapping signals," *Journal of Applied Geophysics*, vol. 61, pp. 292–303, 2007.

[6] Mark Prouty, "Detection and Classification with the MetalMapper™ at Former Camp San Luis Obispo," ESTCP Project No. MM-0603, Geometrics, Inc. July 2009.

[7] I. Shamatava, F. Shubitidze, B. E. Barrowes, J. P. Fernández, K. A. O'Neill, and A. Bijamov, "Live-site UXO classification studies using advanced EMI and statistical models," in R. S. Harmon, J. H. Holloway, and J. T. Broach, eds., *Detection and Sensing of Mines, Explosive Objects, and Obscured Targets XVI, Proceedings of SPIE*8017, 8017-08, (2011).

[8] Shamatava, F. Shubitidze, J. P. Fernández, B. E. Barrowes, K. A. O'Neill, and T. M. Grzegorczyk, "SLO blind data set inversion and classification using physically complete models," in R. S. Harmon, J. T. Broach, and J. H. Holloway, eds., *Detection and Sensing of Mines, Explosive Objects, and Obscured Targets XV, Proceedings of SPIE* 7664, 7664-03 (2010).

[9] F. Shubitidze *et al.*, "Camp Butner UXO Data Inversion and Classification Using Advanced EMI Models," SERDP-ESTCP, Partners 2010.

[10] F. Shubitidze *et al.,* "Camp Beale Live-Site UXO Data Inversion and Classification Using Advanced EMI Models," SERDP-ESTCP, Partners 2011.

[11] F. Shubitidze *et al., "*Advanced EMI models for Camp Beale", ESTCP MR-201101, Demon. Report, http://www.serdp.org/Program-Areas/Munitions-Response/Land/Live-Site-Demonstrations/MR-201101.

[12] F. Shubitidze, B. E. Barrowes, I. Shamatava, J. P. Fernández, T. M. Grzegorczyk, K. O'Neill, and A. Bijamov, "Advanced UXO discrimination: resolving multiple targets and overlapping EMI signals," in R. S. Harmon, J. H. Holloway, and J. T. Broach, eds., *Detection and Sensing of Mines, Explosive Objects, and Obscured Targets XVI, Proceedings of SPIE* 8017, 8017-09 (2011).

[13] A. Bijamov, J. P. Fernández, B. E. Barrowes, I. Shamatava, K. O'Neill, and F. Shubitidze "Camp Butner Live-Site UXO Classification using Hierarchical Clustering and Gaussian Mixture Modeling", IEEE Transactions on Geo-Science and Remote Sensing, Digital Object Identifier 10.1109/TGRS.2013.2287510.

[14] F. Shubitidze, D. Karkashadze, J. P. Fernández, B. E. Barrowes, K. O'Neill, T. M. Grzegorczyk, and I. Shamatava, "Applying a Volume Dipole Distribution Model to Next-

Generation Sensor Data for Multi-Object Data Inversion and Discrimination," *Proceedings of SPIE*, vol. 7664, 2010.

[15] Fridon Shubitidze, Juan Pablo Fernández, Benjamin E. Barrowes, Irma Shamatava, Alex Bijamov, Kevin O'Neill, and David Karkashadze, "The Orthonormalized Volume Magnetic Source Model for Discrimination of Unexploded Ordnance", *IEEE TRANSACTIONS ON GEOSCIENCE AND REMOTE SENSING,* Digital Object Identifier 10.1109/TGRS.2013.2283346.

[16] A. Paski *et al.*, "Former Camp Butner Site Description and EM61 Data Collection and Analysis," SERDP-ESTCP, Partners 2010.

[17] L. Pasion *et al.*, "UXO Discrimination Using Full Coverage and Cued Interrogation Data Sets at Camp Butner, NC," SERDP-ESTCP, Partners 2010.

[18] D. Keiswetter*et al.*, "SAIC Data Analysis of Data Acquired at Camp Butner", , Partners 2010.

[19] S. Billings et al., "Processing and Discrimination Strategies for Next-Generation EMI Sensor Data", SERDP-ESTCP, Partners 2010.

[20] S. Cazares and M. Tuley, "UXO Classification Study: Scoring Memorandum for the former Camp San Luis Obispo, CA," Institute for Defense Analyses, 13 March 2009.

[21] F. Shubitidze, J. P. Fernández, I. Shamatava, A. Luperon, B. E. Barrowes, and K. A. O'Neill, "Inversion-free discrimination of unexploded ordnance in real time," *Proceedings of SPIE* 8357, 8357-04 (2012).

[22]J.-F. Cardoso and A. Souloumiac. "Jacobi angles for simultaneous diagonalization," *SIAM J. Mat. Anal. Appl.*, vol. 17, pp. 161–164, 1996.

[23] J. Byrnes, Ed., *Unexploded Ordnance Detection and Mitigation*, ser. NATO Science for Peace and Security Series B: Physics and Biophysics. Dordrecht: Springer Netherlands, 2009.

[24] J. P. Fernández, F. Shubitidze, I. Shamatava, B. Barrowes, and K. O'Neill, "Realistic subsurface anomaly discrimination using electromagnetic induction and an SVM classifier", Journal in Advanced Signal Processing, 2010.

[25] L. Beran and D.W. Oldenburg, *Selecting a Discrimination Algorithm for Unexploded Ordnance Remediation*. IEEE Transactions on Geoscience and Remote Sensing, 46(9): 2547-2557, 2008.

[26] Zhang, Y., Collins, L., Yu, H., Baum, C. E. and Carin, L., 2003, Sensing of Unexploded Ordnance with Magnetometer and Induction Data: Theory and Signal Processing. *IEEE Trans. Geosci. Remote Sensing,* 41, 1005-1015.

[27] P. Comon, "Independent component analysis, a new concept?" *Signal Processing*, vol. 36, pp. 287–314, 1994.

[28] F. Shubitidze, "A Complex Approach to UXO Discrimination: Combining Advanced EMI Forward Models and Statistical Signal Processing", SERDP Project MR-1572, Final report, January, 2012, http://www.serdp.org/Program-Areas/Munitions-Response/Land/Modeling-and-Signal-Processing/MR-1572.

[29] F. Shubitidze, J. P. Fernández, I. Shamatava, B. E. Barrowes, and K. A. O'Neill, "Joint diagonalization applied to the detection and discrimination of unexploded ordnance," *Geophysics*, Jul 2012, Vol. 77, No. 4, pp. WB149-WB160.

[30] Greg Van, Craig Murray and Steve Saville, "Evaluation of Discrimination Technologies and Classification Results Live Site Demonstration: Former Waikoloa Maneuver Area. ESTCP Project MR-201104, final report. June, 2015.

APPENDICES

Appendix A: Health and Safety Plan (HASP)

As this effort does not involve field data collection, no HASP is required.

Appendix B: Points of Contact

Points of contact (POCs) involved in the demonstration and their contact information are presented in Table 4.

Table 4: Points of Contact for the Advanced EMI Models Demonstration.

POINT OF CONTACT Name	ORGANIZATION Name Address	Phone Fax E-mail	Role in Project
Dr. Fridon Shubitidze	White River Technologies 115 Etna Road Lebanon, NH 03766	Tel: (603) 727-9549 shubitidze@whiterivertech.com	PI
Erik Russell	White River Technologies 115 Etna Road Lebanon, NH 03766	Tel: (603) 678-8386 russell@whiterivertech.com	Project Coordination
Dr. Herb Nelson	ESTCP Program Office 901 North Stuart Street, Suite 303 Arlington, VA 22203-1821	Tel: (571) 372-6400 herb.nelson@nrl.navy.mil	ESTCP Munitions Management Program Manager